15

Thermal properties of glass detectors for heavy ion registration

© E.V. Andreev,[1] P.Y. Apel,[1,2] N.S. Konovalova,[2] N.M. Okateva,[2] N.G. Polukhina,[2] G.T. Sadykov,[2] N.I. Starkov,[2] E.N. Starkova,[2¶] D.M. Strekalina,[2] M.M. Chernyavskiy,[2] T.V. Shchedrina[2]

[1] Joint Institute for Nuclear Research,
141980 Dubna, Moscow oblast, Russia
[2] Lebedev Physical Institute, Russian Academy of Sciences,
119991 Moscow, Russia
[¶] e-mail: starkovaen@lebedev.ru

Received September 14, 2024
Revised October 31, 2024
Accepted November 11, 2024

The results of test studies of various glasses as heavy ion detectors at high temperatures are presented. The samples of the tested glasses were irradiated with heavy ions on the cyclotron U-400 of the Joint Institute for Nuclear Research in Dubna and underwent thermal treatment in a muffle furnace. Glass etching and data analysis were carried out in the Laboratory of Elementary Particles of the LPI. The search and analysis of etched tracks was carried out on an automated measuring complex PAVICOM under an optical microscope. Two out of five tested glasses were selected for further research.

Keywords: glass detectors for registration of heavy ions, testing of glasses with different compositions, annealing at high temperatures, image processing on an automated microscope.

DOI: 10.61011/TP.2025.01.60524.272-24

Introduction

Synthetic and natural dielectrics, in particular glass and mica, are commonly used in various fields of science and technology, including experimental nuclear physics. The applicability of various glasses for the recording of superheavy nuclei and their decay products is studied in this paper.

Superheavy chemical elements are produced at accelerators as a result of the complete fusion of the target nucleus and the incident particle [1–3]. Experiments for the synthesis of superheavy elements are successfully conducted, in particular, at Flerov Laboratory of Nuclear Reactions of the Joint Institute for Nuclear Research (JINR FLNR) [4]. Elements from 114 (flerovium) to 118 (oganeson) were obtained in the FLNR experiments by the interaction of accelerated ^{48}Ca ions with actinide targets, from plutonium to californium [5]. Elements with a large atomic number should be used as a projectile and target to obtain elements heavier than oganeson (for example, the reaction of the chromium isotope ^{54}Cr with a curium target ^{96}Cm is considered to obtain the 120-th element). JINR has created a Factory of Superheavy Elements to synthesize and study the properties of superheavy elements (cyclotron DTs-280, gas-filled separators of recoil cores GRAND and DGFRS-II) [6], which was commissioned in 2020.

A beam of incoming heavy ions passes through the target and reaches the separator in experiments for the synthesis of superheavy elements in the accelerator. A new nucleus is formed in the separator, the trajectory of which coincides with the direction of the beam, it is separated from other nuclides (the initial beam and other reaction products) and transmitted to the detector. Superheavy isotopes with a core charge of more than 112, obtained by the hot fusion method, are recorded using a detector that records the time of entry into the detector and the coordinates of implanted recoil nuclei, the energies of α-particles of decay and fission products. The transfer takes about 10^{-6} s and the core should exist for at least this time for detection [7]. A synthesized chemical element is recognized as detected if its core has not decayed during 10^{-14} s [8].

The requirements for the separation of reaction products, in particular, a speed commensurate with the lifetime of the isolated nuclide, are provided by the method of gas thermochromatography, which involves chemical processes in a gaseous medium [9]. Gas-chemical methods of separation of elements are based on the transfer of a radionuclide from a gaseous to a condensed phase. Conditions are created in the process of gas chemical separation of elements, when the elements are in different chemical forms, in particular due to changes of the temperature of the carrier gas. The gas thermochromatography is used to separate elements with similar properties, which precipitates substances on a column with a temperature gradient [10]. For elements heavier than 112, the transition from sorption to desorption may lie in the temperature range above 200°C. At such temperatures, the use of semiconductor detectors and nuclear emulsion is impossible, and only dielectric track detectors [11] can be used for these purposes. However, annealing (complete or partial disappearance) of ion tracks can occur at high temperatures in dielectric detectors [12]. The degree of annealing depends on the temperature and time of thermal exposure in addition to the properties of the detector.

Table 1. Stages of heat treatment of irradiated glasses

Temperature	Interval 1 (uniform heating)	Interval 2 (process stabilization)	Interval 3 (holding at constant temperature)	Interval 4 (cooling in furnace)
Up to 300°C	25–285°C (90 min)	285–300°C (30 min)	300°C (180 min)	∼ 6 h
Up to 300°C	–	–	300 ± 8°C (10 min)	–
Up to 500°C	25–475°C (135 min)	475–500°C (30 min)	500°C (180 min)	∼ 8 h
Up to 500°C	–	–	500 ± 10°C (10 min)	–

The Laboratory of Elementary Particles of Lebedev Physical Institute of Russian Academy of Science (LPI) studies various dielectric materials for recording superheavy nuclei and their decay products in a thermochromatographic column at the JINR Superheavy Elements Factory at high temperatures. Glass samples were irradiated with heavy ions in the ion transport channel of the resonant cyclic accelerator U-400 in the test experiments. All samples were irradiated with xenon ions accelerated to an energy of 475 MeV; samples of quartz glass KU-2 were also irradiated on a beam with an energy of 160 MeV. A muffle furnace with a programmable heating algorithm was used for heat treatment of irradiated glasses. A two-stage warm-up mode was used to avoid overheating above the preset level for prolonged exposures (∼ 180 min) (first, rapid heating, then a slower heating to the desired temperature). The stages of heat treatment of irradiated glasses are presented in Table 1.

This paper presents the results of the analysis of annealed and non-annealed glass samples with different compositions irradiated with heavy ions at the JINR accelerator.

Chemical etching may result in tracks on the surface of the samples, visible through an optical microscope. The dimensions of the projection of the track onto the plane of the glass surface are determined using programs developed in the LPI Laboratory of Elementary Particles for image processing using a high-tech automated microscope. The image of the track projection on the glass surface is approximated by an ellipse when analyzing the data (the major and minor axes of the ellipse are further referred to in the text as the length and width of the track projection, respectively). The projection width of the track is related to the etching of the channel walls and characterizes the etching rate of the base material, and the projection length characterizes the etching rate along the track, i.e. in the area damaged by the passage of a charged particle, and is related to the properties of this particle. The ion path to a stop in the detector material is calculated based on the size of the projection highlighted in the image [13]. Measurements and automatic data recording are conducted using PAVICOM installation [14].

1. Phosphate glasses

Samples of phosphate-based „strong erbium laser glass" (Strong Erbium Laser Glass, SELG) were tested [15]. The high content of aluminum and boron oxides in glass ensures its mechanical strength, chemical resistance, and refractory properties. The deformation temperature of the glass is 755°C.

Four SELG phosphate glass samples were selected for irradiation with xenon ions $^{132}Xe^{26+}$ with an energy of 475 MeV. The samples were treated in 40% solution of hydrofluoric acid HF after irradiation.

SELG samples № 1 and № 2 were not subjected to temperature annealing and were etched from 10 to 150 min in 20 min increments. Visible tracks appeared after 60 (sample № 1) and after 70 (sample № 2) min of etching. Fig. 1 showing the images of a single field of view of the surface of samples № 1 (Fig. 1, *a*–*c*) and № 2 (Fig. 1, *d*–*f*), illustrates the dynamics of track size changes at different etching stages. The reason for the delay of the appearance of tracks is still unclear, but similar effects have been observed on samples of other glasses. This may be attributable to the fact that in the first steps of etching, the etching speed of the glass itself is greater than the etching speed of the track, which disappears in the etched layer. Traces appear later when the etching speed of the glass itself becomes less than the etching speed of the track.

Fig. 2 shows the results of measurements of track sizes in non-annealed SELG phosphate glass samples № 1 and № 2 depending on the etching time.

The particle stopping in the detector is indicated by a kink in the curve showing the dependence of the track projection length on the etching time, when the etching process moves from the track area to the base material. These are 100 (fig. 2, *a*) and 120 min in Fig. 2 (Fig. 2, *b*). It is necessary to know the size of the layer etched from the sample surface to determine the length of the ion track before stopping. The size of the etched layer is determined by weighing the sample at each etching step [13]. The weight change of the sample can be comparable to the weighing accuracy (0.1 mg) at a low etching rate, which leads to sufficiently

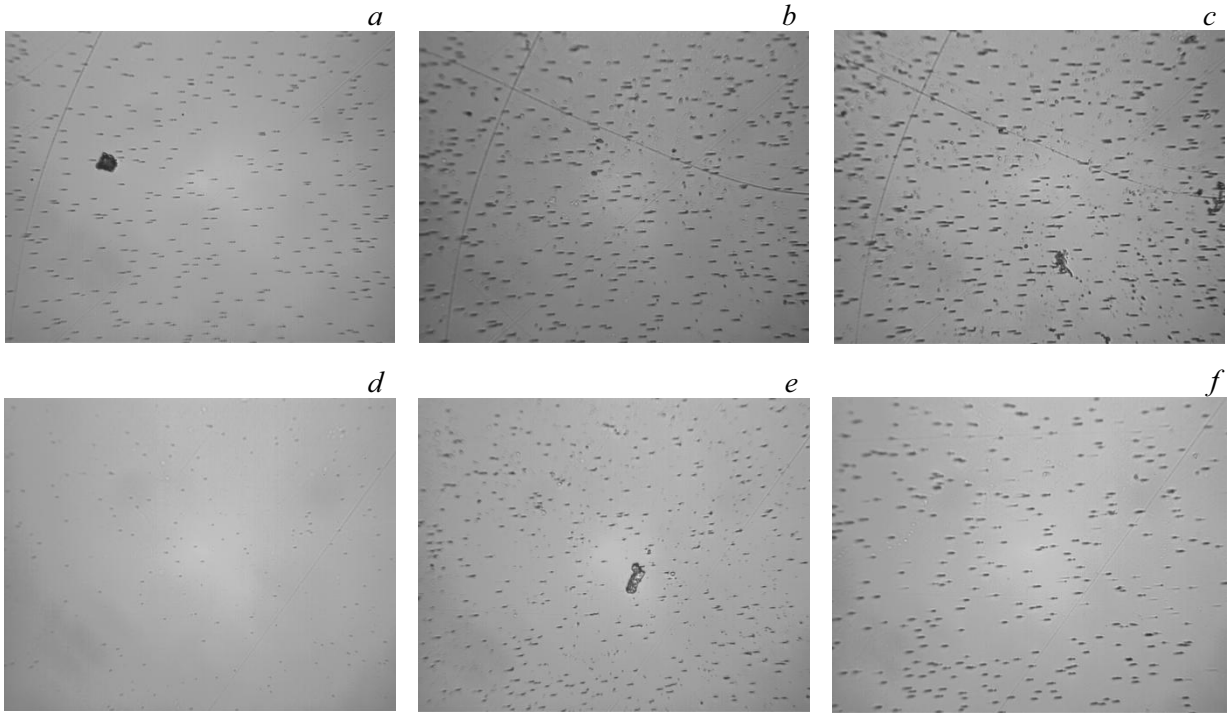

Figure 1. Cluster size variation in SELG phosphate glass samples. Etching time of non-annealed samples: 1 — 100 (it a), 135 (*b*), 155 (*c*) and № 2 — 70 (*d*), 120 (*e*), 160 min (*f*). Size of one field of view 280 × 220 μm.

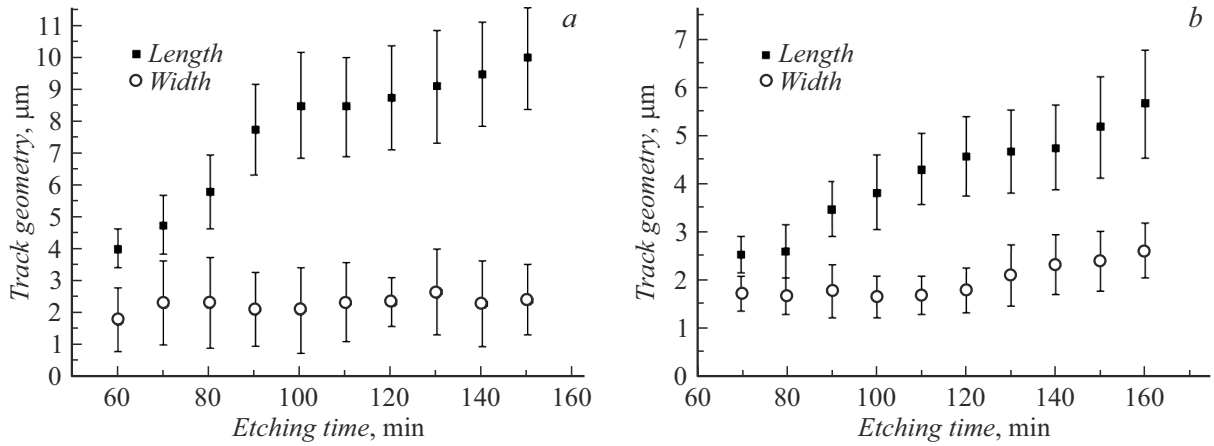

Figure 2. The sizes of etched tracks in samples № 1 (*a*) and № 2 (*b*) made of SELG phosphate glass, depending on the etching time in 40% HF.

large errors in the measured value of the etched layer. A more reliable result is achieved when measuring the etching rate of glass over a long period of time (more than 100 min), when the weight change of the sample exceeds 0.5 mg, i.e. $\sim 0.2\%$ of sample weight. Fig. 3 shows graphs of the SELG phosphate glass etching rate of for samples № 1 and № 2.

SELG№ 3 and № 4 glass samples irradiated with xenon ions were annealed at temperatures of 300 (sample № 3) and 500°C (sample № 4). The result was the destruction of the surface of sample № 4 and the absence of etched channels visible under an optical microscope in sample № 3. The etching rate of the material turned out to be comparable to the average etching rate of non-annealed samples, approximately 0.8−0.9 μm/h (Fig. 4).

It is possible to make a qualitative comparison of the results obtained with the results of etching phosphate glasses KNFS-3 (a direct comparison is not possible since KNFS-3 was etched in 20%≈). Two sections can be distinguished on the graph of the dependence of the length of the track projection on the time of etching of glasses KNFS-3: steeper at the beginning of etching, and more gentle after 100−120 min of etching [13]. This is attributable to the

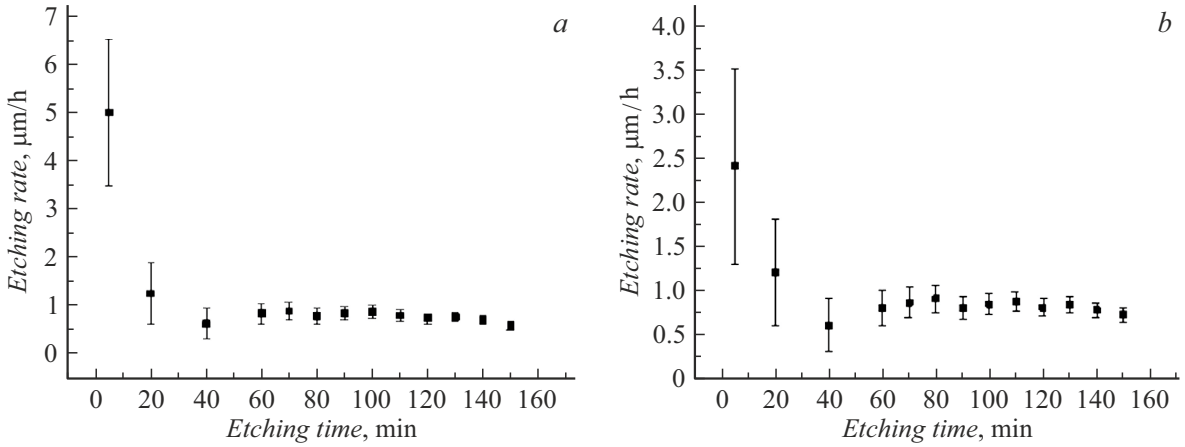

Figure 3. SELG phosphate glass etching rate: *a* — sample № 1; *b* — sample № 2.

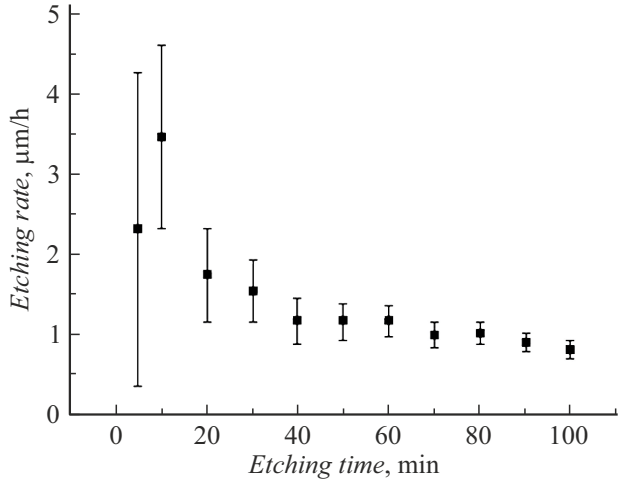

Figure 4. Etching rate of the annealed SELG phosphate glass sample № 4 (annealing temperature 500°C).

higher etching rate in the track area compared to the etching rate of the bulk of the glass. The rate of change of the length of the etched channel decreases after 100−120 min of etching (as the ion approaches the stopping point in the glass). Depending on the track length and etching time obtained for non-annealed SELG phosphate glasses, two sections and a change of slope from steeper to more gentle in the region of 100−120 min etching are also visible, however, in this case, the etching rate in the track area is several times lower. Unlike SELG phosphate glasses, the post-etching annealing of glasses KNFS-3 at a temperature of 300°C did not lead to the disappearance of tracks, but only to a decrease of their geometric dimensions [16].

2. Aluminum-calcium glass

Aluminum-calcium glass AKS5 is produced by Lytkarino Optical Glass Plant (LOGP) [17]; aluminum oxide is used as the glass-forming substance. AKS5 glass is characterized by high temperature resistance and good mechanical properties, the annealing temperature is $680 \pm 10^{P}\circ$, the deformation temperature is 780°C, the heat resistance is 90°C. The developed technological process makes it possible to obtain samples with a thickness of 3 mm, which is associated with the high crystallization ability of glass.

Some of the irradiated samples of glass AKS5 were annealed after irradiation at a temperature of 300°C. The samples did not change shape and did not have any visible damage as a result of annealing. Etching of the irradiated samples in HF (the samples were etched at concentrations of 10, 20, and 40%) did not result in visible tracks, and the surface of the samples was destroyed by acid. Fig. 5 shows the etching rates of non-annealed and annealed samples in hydrofluoric acid of different concentrations.

One sample was etched in orthophosphoric acid H_3PO_4, which actively interacts with Al, which is a component of AKS5. Fig. 6 shows the etching rate of the sample in orthophosphoric acid with a concentration of 85%, depending on the etching interval.

The etching rate of glass treated by nitric acid (concentration 65%) was 8 μm/h, etching rate of glass treated by hydrochloric acid (concentration 36%) was 45 μm/h. There were no visible ion tracks in the aluminum-calcium glass after all types of treatment.

3. Quartz glass

Quartz glass or optical fused quartz is a single-component glass consisting of almost pure silica (silicon dioxide SiO_2) in an amorphous form. Quartz glass is characterized by high mechanical strength, significantly exceeding the strength of other optical materials, high uniformity and thermal resistance; the annealing temperature is higher than 1000°C. The properties of quartz glass are described in more detail in Ref. [18].

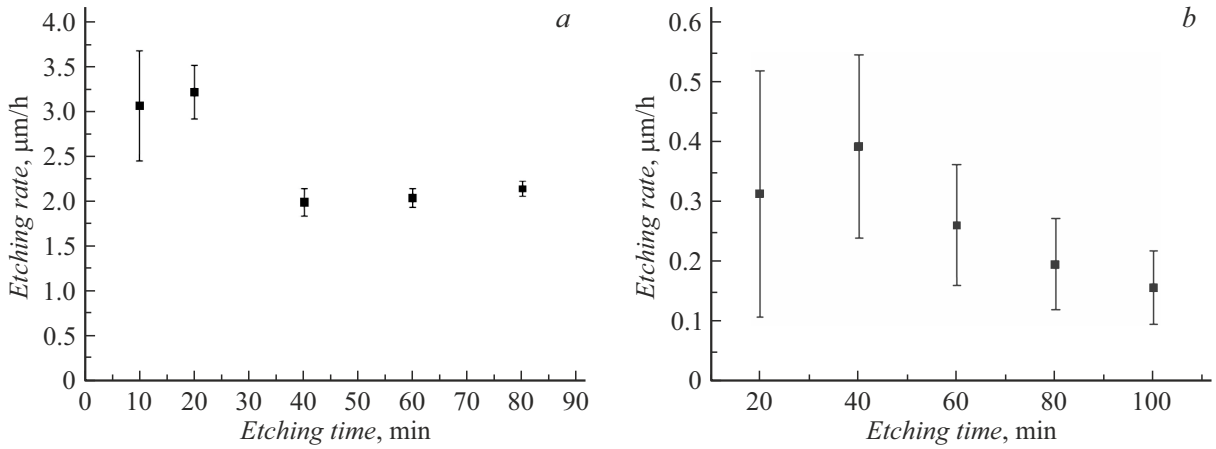

Figure 5. Etching rate of glass AKS5: *a* — etching of a non-annealed sample in 40% HF; *b* — etching of sample annealed at 300°C, in 10% HF.

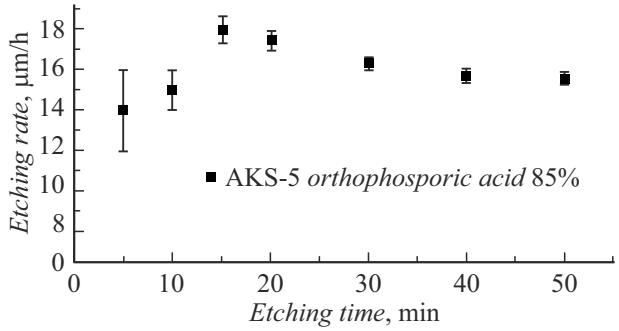

Figure 6. Etching rate of a sample of glass AKS5 etched in 85% solution of orthophosphoric acid H_3PO_4.

The samples of quartz glass KU-2 which has high infusibility, were tested. The results of testing of samples without annealing showed that this glass is suitable for determining the charge by the etching rate of tracks of different nuclei at a fixed energy per nucleon [18].

In further studies, samples of quartz glass KU-2 were irradiated using isochronous cyclotron U-400 of JINR FLNR, designed to produce beams of accelerated ions with atomic mass in the range $A = 4-209$ and energy of 3–29 MeV/nucleon. The irradiation was performed using Xe ion beam at an angle of 45° with two beam energy values — 160 and 475 MeV. During some irradiation of samples with ions with an energy of 160 MeV, a layer of a PET absorber was placed in front of the glass target for collecting the energy of incident ions of 80 MeV.

Table 2 shows the values of the Xe ion path in glass KU-2 with these energies, obtained using the SRIM program [19], and the results of measurements in non-annealed samples.

The irradiated samples were etched in a 2% solution of hydrofluoric acid HF, the etching time was about 200 min with increments of 10 min.

Fig. 7 shows photographs of tracks on the glass surface after etching for 75 min with different values of beam energy and the results of cluster isolation obtained after processing on PAVICOM installation. It can be seen that the radiation dose $10^5\,\mathrm{cm}^{-2}$ with an energy of 475 MeV (Fig. 7, *c,f*) is too high, since the tracks quickly spread out and overlap each other (radiation density is of great importance when studying the possibility of track identification).

Fig. 8 shows the values of the track projection lengths L_{pr} onto the glass surface depending on the etching time t, obtained taking into account the thickness of the etched layer.

The inflection of the function $L_{pr}(t)$ indicates the transition from etching ion-damaged areas of the material to etching undamaged glass [18]. The inflection points in Fig. 8 correspond to 135, 120, and 100 min for energies of 80, 160, and 475,MeV, respectively. Data on the length of the track projection before stopping (Table 2) allow obtaining the dependence of the etching rate on the ion energy (Fig. 9). For instance, the etching rate of ion tracks with an energy of 160 MeV is consistent with the value $11.2 \pm 0.6\,\mu$m/h obtained in Ref. [18]. An algorithm for determining charge from the etching rate of tracks for different ions at a fixed energy per nucleon was discussed earlier in Ref. [13].

Two samples of glass KU-2, irradiated with Xe ions with an energy of 475 MeV, were annealed at temperatures of 300 and 500°C in muffle furnace of FLNR (Table 1). Fig. 10, *a* shows the dependence of the track projection length in the annealed sample on the etching time. The inflection point on the graph corresponds to the etching time of 100 min and the track projection length of $\sim 10 \pm 1.1\,\mu$m. The annealing of at a temperature of 500°C reduces the etching rate of samples irradiated with ions with an energy of 475 MeV in the track region by more than three times compared with non-annealed samples (Fig. 9); at the same time, the etching rate of the base material remains the same after annealing.

Fig. 10 shows the etching rates of a non-annealed sample of quartz glass KU-2 (Fig. 10, *b*) and a sample annealed at a temperature of 500°C (Fig. 10, *c*). It can be seen that

Table 2. Calculated and measured parameters of Xe ion tracks in quartz glass KU-2

Energy, MeV	80	160	475
Path of core Xe, μm (SRIM)	13.5	18.5	37
Stop point, min	135	120	100
Length of the projection to stop point, μm	4.5 ± 0.5	8 ± 0.8	16 ± 1.2
Thickness of etched layer, μm	7.3 ± 0.3	7.2 ± 0.3	7 ± 0.3
Full track length, μm	16.5 ± 1.7	21 ± 1.9	32.5 ± 2.5
Track rate of etching, μm/h	7.3 ± 0.8	10.5 ± 0.8	19.5 ± 1.2

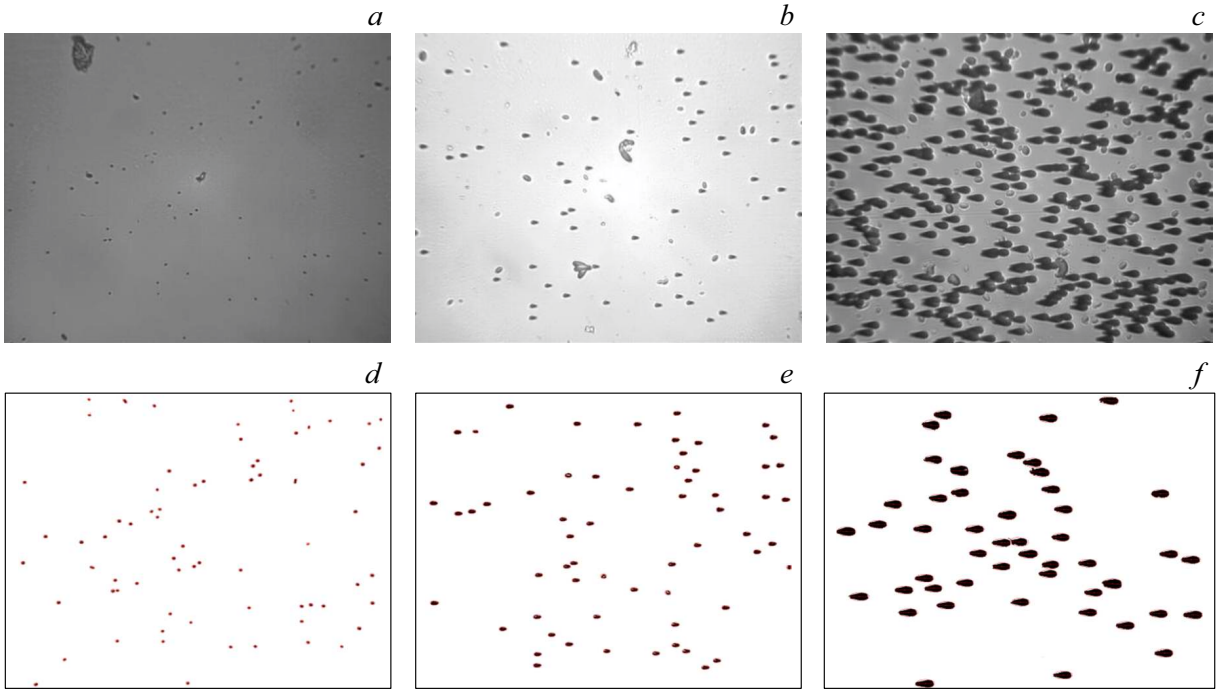

Figure 7. Top row: photos of traces of nuclei with energies 80(a), 160 (b) and 475 MeV (c) after etching for 75 min in 2%HF. Bottom row: images of selected clusters corresponding to ion energies of 80 (d), 160 (e) and 475 MeV (f) (the result of processing on PAVICOM).

the etching rate is not constant and exhibits a sharper drop in the annealed sample with the increase of the etching time, compared with the non-annealed sample. Thus, the tracks remain even when annealed for 10 h at a temperature of 500°C in quartz glass KU-2, but they change their characteristics. This circumstance should be taken into account when using glass of this brand as a detector.

4. Silicate glass S48-3

Silicate glass S48-3 (produced by the Lytkarino Optical Glass Plant) was tested, its samples were etched in solutions of hydrofluoric, nitric, hydrochloric and orthophosphoric acids of the same concentration. Hydrofluoric acid destroyed the surface of the sample; the remaining acids did not interact with the sample: no weight change was observed, the surface was not destroyed. Visible tracks were not detected in any of the etched samples.

Conclusion

The paper presents the results of studies of glasses with different chemical compositions for use as heavy ion

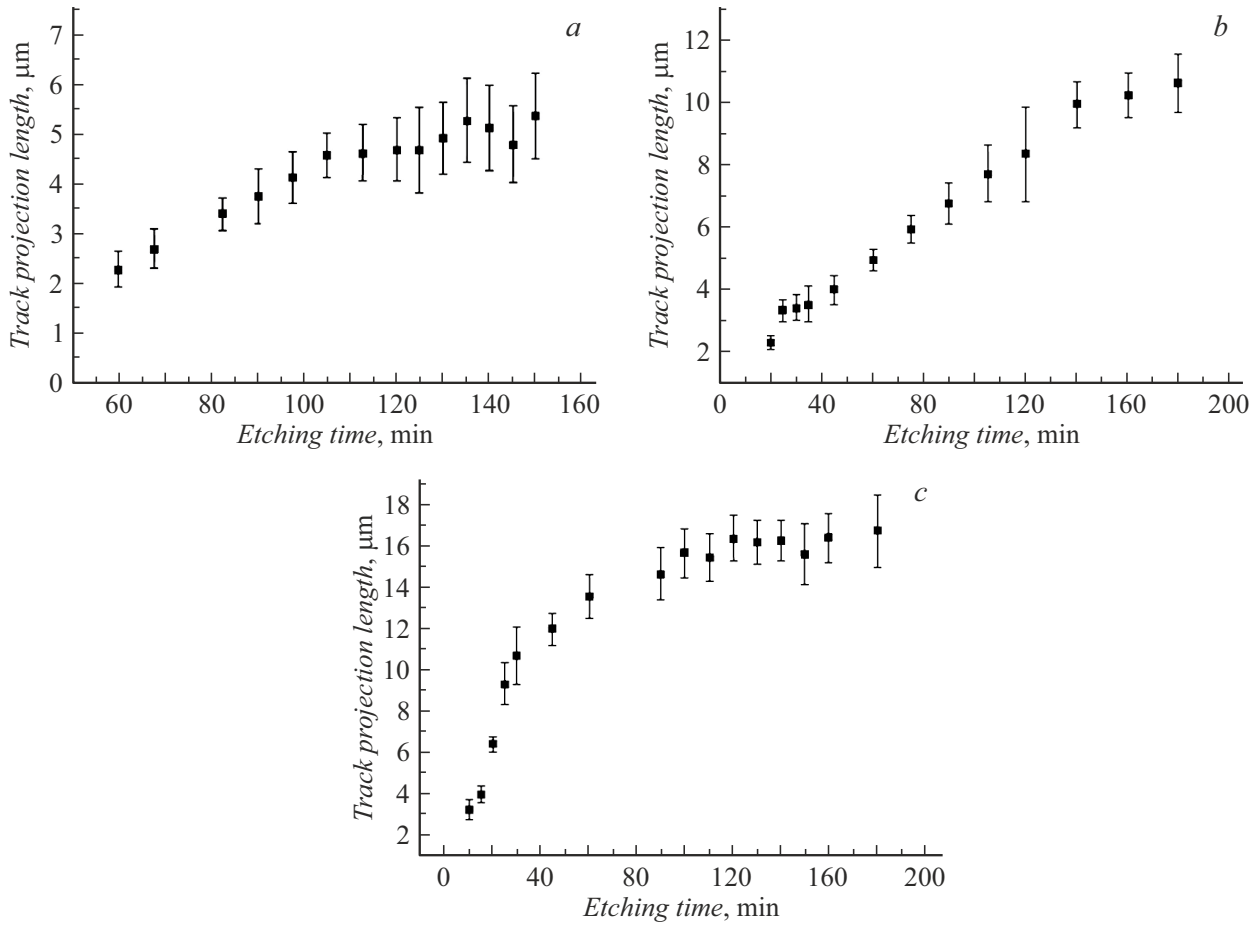

Figure 8. Dependence of the length of the track projection on the glass surface on the etching time (function $L_{pr}(t)$) with beam energy of 80 (a), 160 (b) and 475 MeV (c).

detectors at high temperatures. According to the results, the tested glasses can be divided into several categories.

— Glasses in which visible tracks were not detected by an optical microscope in any treatment conditions, both with and without heating (aluminum-calcium glass AKS5 and silicate glass S48-3).

— Phosphate glasses in which, as a result of treatment at room temperature, tracks were detected, but when the samples were annealed after irradiation, either the tracks were not observed (SELG glass) or the geometric parameters significantly changed (glass KNFS-3). The characteristics of the tracks exhibited weak changes on the irradiated heated samples of KNFS-3.

— Quartz glass KU-2, in which tracks were observed under all treatment conditions. The tracks survived in the quartz glass while annealing after irradiation, but changed their geometric characteristics (requires further studies). The next stage of quartz glass testing involves the study of samples of KU-2 irradiated in a heated state.

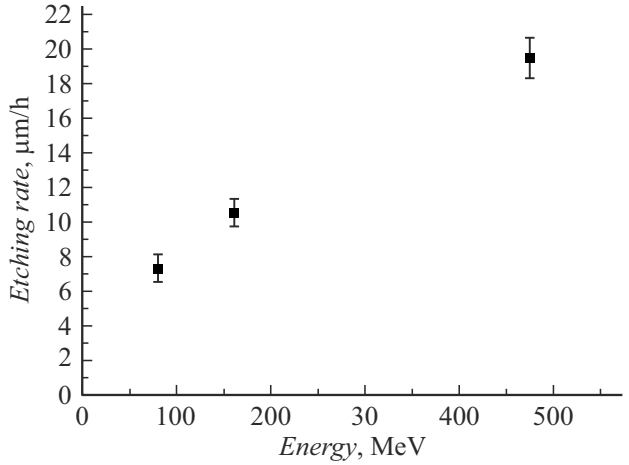

Figure 9. Dependence of the etching rate of tracks in quartz glass KU-2 on the energy of Xe ions.

Thus, at this stage of study, phosphate glass KNFS-3 and quartz glass KU-2 seem to be applicable as heavy ion detector materials at the JINR Superheavy Elements Factory, but require further testing. SELG glass requires additional studies for the analysis of temperature effects in various conditions.

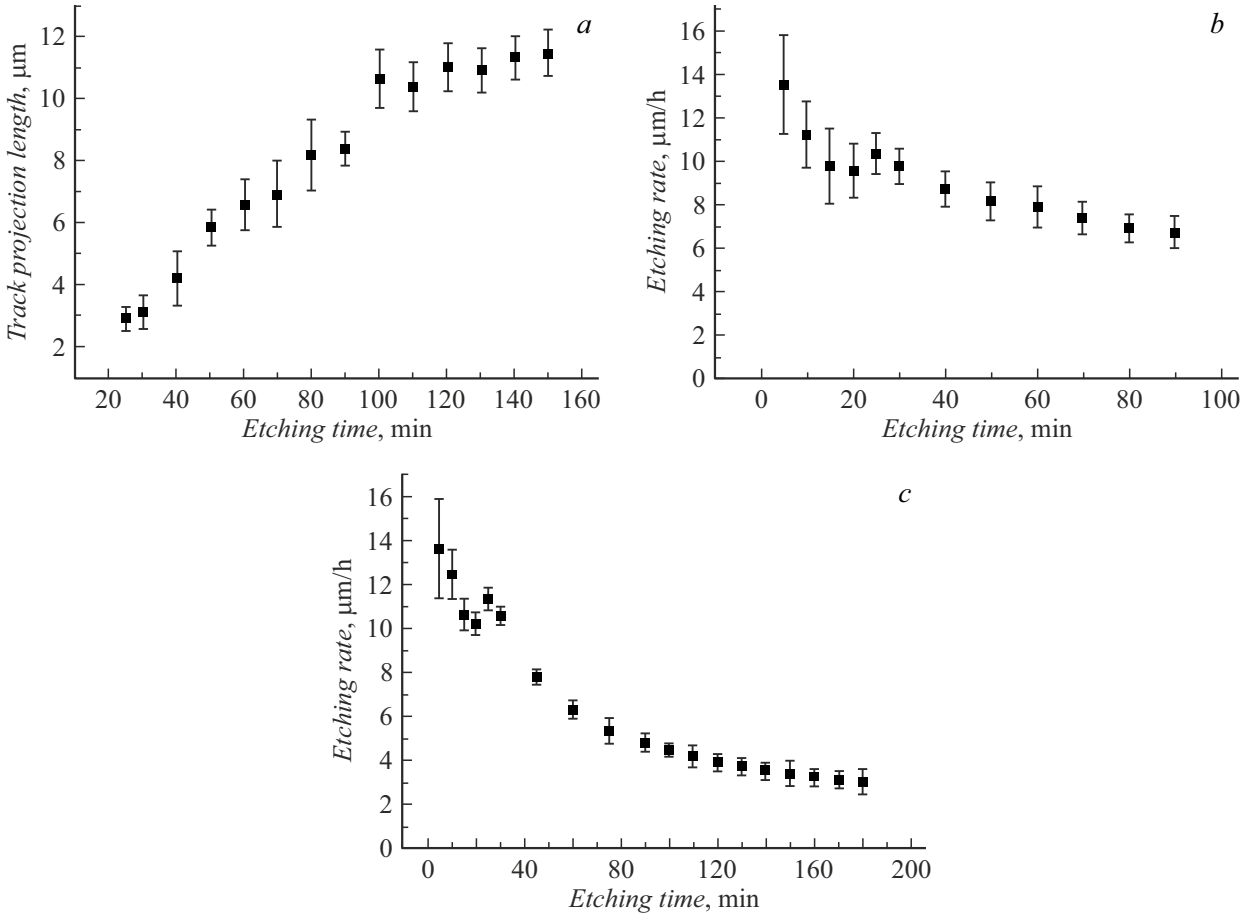

Figure 10. *a* — dependence of the track projection length on the etching time for sample of glass KU-2 annealed at a temperature of 500°C; *b* — etching rate of non-annealed glass KU-2, sample № 1; *c* — Etching rate of glass KU-2 annealed at 500°C, sample No. 2.

Funding

The work was supported by the Russian Science Foundation under the program „Conducting basic scientific research and exploratory scientific research by individual scientific groups“ (project № 23-12-00054).

Conflict of interest

The authors declare that they have no conflict of interest.

References

[1] V.V. Volkov. *YAdernye reakcii glubokoneuprugih peredach* (Energoizdat, M., 1982) (in Russian).

[2] Yu.Ts. Oganessian, A. Sobiczewski, G.M. Ter-Akopian. Phys. Scr., **92**, 023003 (2017). DOI: 10.1088/1402-4896/aa53c1

[3] B.S. Ishkhanov, T.Y. Tretyakova. Vestnik Moskovskogo un-ta, seriya 3: Fizika, astronomiya **3**, 3 (2017) (in Russian).

[4] Yu.Ts. Oganessian, U.K. Utyonkov. Rep. Prog. Phys., **78**, 036301 (2015). DOI: 10.1088/0034-4885/78/3/036301

[5] Yu.Ts. Oganessian, V.K. Utyonkov, D. Ibadullayev, F.Sh. Abdullin, S.N. Dmitriev, M.G. Itkis, A.V. Karpov, N.D. Kovrizhnykh, D.A. Kuznetsov, O.V. Petrushkin, A.V. Podshibiakin, A.N. Polyakov, A.G. Popeko, R.N. Sagaidak, L. Schlattauer, V.D. Shubin, M.V. Shumeiko, D.I. Solovyev, Ys.S. Tsyganov, A.A. Voinov, V.G. Subbotin, A.Yu. Bodrov, A.V. Sabelnikov, A. Lindner, K.P. Rykaczewski, T.T. King, J.B. Roberto, N.T. Brewer, R.K. Grzywacz, Z.G. Gan, Z.Y. Zhang, M.H. Huang, H.B. Yang. Phys. Rev. C, **106** (2), 026412 (2022). DOI: 10.1103/PhysRevC.106.024612

[6] S. Dmitriev, M. Itki, Y. Oganessian. EPJ Web Conf., **131**, 08001 (2016). DOI: 10.1051/epjconf/201613108001

[7] V. Zagrebaev, A. Karpov, W. Greiner. J. Phys.: Conf. Ser., **420**, 012001 (2013). DOI: 10.1088/1742-6596/420/1/012001

[8] R.C. Barber, P.J. Karol, H. Nakahara, E. Vardaci, E.W. Vogt. Pure Appl. Chem., **83** (7), 1485 (2011). DOI: 10.1351/PAC-REP-10-05-01

[9] T.S. Zvarova, I. Zvara. *Razdelenie transuranovykh elementov pri pomoshchi gazovoj hromatografii khloridov* (R6-4911, Ob'edin. in-t yadernykh issledovanij, Dubna, 1970) (in Russian).

[10] B.L. Zhuikov. *Metody razdeleniya letuchikh elementov i oksidov v poiske sverhtyazhelykh elementov i pri poluchenii radioizotopov* (Avtoref. kand. diss., MGU, M., 1982) (in Russian).

[11] R.L. Fleisher, P.B. Price, R.M. Wolker. *Nuclear tracks in solids* (Washington University, St. Louis, University of California Press, 1975)

[12] S.A. Durrani, R.K. Bull. *Solid state nuclear track detection: Principles, methods and applications* (Pergamon Press, Oxford, NY., 1987)
[13] N. Burtebayev, K. Argynova, M.M. Chernyavskiy, A.A. Gippius, G.V. Kalinina, N.S. Konovalova, T.N. Kvochkina, M. Nassurlla, N.M. Okateva, A. Pan, N.G. Polukhina, Zh.T. Sadykov, T.V. Shchedrina, N.I. Starkov, E.N. Starkova, I.I. Zasavitskii. Bull. Lebedev Phys. Inst., **49** (10), 350 (2022). DOI: 10.3103/S1068335622100062
[14] A. Alexandrov, N. Konovalova, N. Okateva, N. Polukhina, N. Starkov, T. Shchedrina. Measurement, **187**, 110244 (2022). DOI: 10.1016/j.measurement.2021.110244
[15] G. Karlsson, F. Laurell, J. Tellefsen, B. Denker, B. Galagan, V. Osiko, S. Sverchkov. Appl. Phys. B, **75**, 1 (2002). DOI: 10.1007/s00340-002-0950-4
[16] N. Burtebaev, K. Argynova, M.M. Chernyavskiy, A.A. Gippius, N.S. Konovalova, T.N. Kvochkina, M. Nasurlla, N.M. Okateva, A.N. Pan, N.G. Polukhina, Zh.T. Sadykov, T.V. Shchedrina, N.I. Starkov, E.N. Starkova, I.I. Zasavitsky. J. Exp. Theor. Phys., **134**, 528 (2022). DOI: 10.1134/S1063776122040033
[17] L.I. Avakyants, A.N. Ignatov, E.Yu. Krekhova, V.I. Molev, A.E. Pozdnyakov, S.N. Sizov, V.F. Surkova. J. Opt. Technol., **80** (4), 204 (2013). DOI: 10.1364/JOT.80.000204
[18] P.Yu. Apel, M.M. Chernyavskiy, A.A. Gippius, G.V. Kalinina, N.S. Konovalova, N.M. Okateva, N.G. Polukhina, Zh.T. Sadykov, T.V. Shchedrina, N.I. Starkov, E.N. Starkova, I.I. Zasavitskii. Bull. Lebedev Phys. Inst., **51** (4), 117 (2024). DOI: 10.3103/S1068335624600062
[19] J.F. Ziegler. Nucl. Instrum. Methods Phys. Res. B, **219**–**220**, 1027 (2004). DOI: 10.1016/j.nimb.2004.01.208

Translated by A.Akhtayamov